Physical exertion exacerbates decline in the musculature of an animal model of Duchenne muscular dystrophy

K. J. Hughes[a], A. Rodriguez[a], K. M. Flatt[b], S. Ray[c,1], A. Schuler[a], B. Rodemoyer[a], V. Veerappan[a], K. Cuciarone[a], A. Kullman[a], C. Lim[a], N. Gutta[a], S. Vemuri[a], V. Andriulis[a], D. Niswonger[a], L. Barickman[a], W. Stein[a], A. Singhvi[c], N. E. Schroeder[b], and A. G. Vidal-Gadea[a,2]

[a]School of Biological Sciences, Illinois State University, Normal, IL 61790; [b]Department of Crop Sciences, University of Illinois at Urbana–Champaign, Urbana, IL 61801; and [c]Division of Basic Sciences, Fred Hutchinson Cancer Research Center, Seattle, WA 98109

Edited by Iva Greenwald, Columbia University, New York, NY, and approved January 9, 2019 (received for review July 6, 2018)

Duchenne muscular dystrophy (DMD) is a genetic disorder caused by loss of the protein dystrophin. In humans, DMD has early onset, causes developmental delays, muscle necrosis, loss of ambulation, and death. Current animal models have been challenged by their inability to model the early onset and severity of the disease. It remains unresolved whether increased sarcoplasmic calcium observed in dystrophic muscles follows or leads the mechanical insults caused by the muscle's disrupted contractile machinery. This knowledge has important implications for patients, as potential physiotherapeutic treatments may either help or exacerbate symptoms, depending on how dystrophic muscles differ from healthy ones. Recently we showed how burrowing dystrophic (*dys-1*) *C. elegans* recapitulate many salient phenotypes of DMD, including loss of mobility and muscle necrosis. Here, we report that *dys-1* worms display early pathogenesis, including dysregulated sarcoplasmic calcium and increased lethality. Sarcoplasmic calcium dysregulation in *dys-1* worms precedes overt structural phenotypes (e.g., mitochondrial, and contractile machinery damage) and can be mitigated by reducing calmodulin expression. To learn how dystrophic musculature responds to altered physical activity, we cultivated *dys-1* animals in environments requiring high intensity or high frequency of muscle exertion during locomotion. We find that several muscular parameters (e.g., size) improve with increased activity. However, longevity in dystrophic animals was negatively associated with muscular exertion, regardless of effort duration. The high degree of phenotypic conservation between dystrophic worms and humans provides a unique opportunity to gain insight into the pathology of the disease as well as the initial assessment of potential treatment strategies.

muscular dystrophy | *C. elegans* | degeneration | exercise | hypertrophy

Duchenne muscular dystrophy (DMD) is a lethal muscle-wasting disease affecting 1 in 3,500 males. It is characterized by progressive muscle weakness, loss of ambulation, and premature death (1). To date there is no cure for DMD, which is caused by loss-of-function mutations in the gene encoding the dystrophin protein, resulting in its absence from muscles (2). At the sarcolemma, dystrophin links cytoskeleton to the extracellular matrix through a complex of membrane proteins, where it helps protect myocytes from the forces generated by their contractile machinery. Additionally, dystrophin participates in nitric oxide signaling cascade (3). Absence of dystrophin may cause muscle shearing and increased sarcoplasmic calcium levels, potentially leading to muscle decline directly through cytotoxicity (4), mitochondrial damage (5), or additional mechanisms (6).

DMD patients display dramatic muscle degeneration and lose mobility early on in life (1). Progress in DMD research is hindered by lack of genetic model systems that accurately recapitulate the severe loss of mobility and muscle degeneration seen in humans. While similar deficits are observed in canine models (7), genetically amenable organisms such as flies, worms, and mice have not matched this phenotypic severity (8–10). However, progress has resulted from matching dystrophin mutations with sensitizing mutations in related proteins (or through other insults) that more closely recapitulate the acute motor and muscular decline seen in humans (11). While useful, these approaches also cloud interpretation of their results because the direct link between phenotype and loss of dystrophin is missing. Lack of phenotypic severity in these systems may result from compensatory mechanisms (12, 13), and/or short life span. Alternatively, attenuated phenotypes may result from insufficient muscular challenge to animals that are (mostly) kept under low exertion regimens not matching those in their natural environment. Consistent with this idea, muscle degeneration was directly correlated with muscle strength in DMD mice (14). This suggests that modeling the disease accurately requires appropriate behavioral paradigms capable of modulating muscle exertion in behaving animals.

Another unanswered aspect of DMD is the sequence of molecular steps linking loss of dystrophin to myocyte degeneration. It is now widely agreed that myofiber death is mediated by aberrant increases in sarcoplasmic calcium entering through the sarcolemma (15). The mechanism linking sarcolemma stress and calcium entry remain unresolved but may involve the X–reactive oxygen species pathway (16), receptor-operated calcium entry

Significance

Duchenne muscular dystrophy is a degenerative disease affecting tens of thousands of people in the United States alone. Much remains unknown about the disease, including the chain of events that links the loss of dystrophin to muscle death, and the extent to which exercise might be able to protect degenerating muscles. We used the nematode *Caenorhabditis elegans* to show that sarcoplasmic calcium dysregulation takes place in dystrophic muscles before other overt signs of damage manifest. When placed in assays that altered muscular activity by increasing either contraction frequency or amplitude, we observed several metrics associated with muscular repair increase. However, no treatment positively affected the life expectancy of dystrophic animals.

Author contributions: K.J.H., A.R., K.M.F., S.R., A. Singhvi, N.E.S., and A.G.V.-G. designed research; K.J.H., A.R., K.M.F., S.R., A. Schuler, B.R., K.C., A.K., C.L., N.G., S.V., V.A., L.B., and A.G.V.-G. performed research; A. Singhvi, N.E.S., and A.G.V.-G. contributed new reagents/analytic tools; K.J.H., A.R., K.M.F., A. Schuler, B.R., V.V., C.L., N.G., S.V., V.A., D.N., W.S., N.E.S., and A.G.V.-G. analyzed data; and K.J.H., W.S., and A.G.V.-G. wrote the paper.

The authors declare no conflict of interest.

This article is a PNAS Direct Submission.

[1]Present address: Program in Neuroscience, University of Washington, Seattle, WA 98195.

[2]To whom correspondence should be addressed. Email: avidal@ilstu.edu.

This article contains supporting information online at www.pnas.org/lookup/suppl/doi:10.1073/pnas.1811379116/-/DCSupplemental.

Published online February 12, 2019.

channels (17), or phosphorylation of transient receptor potential cation channels (18). Understanding the proximal cause of increased calcium levels in DMD muscles remains an important goal.

At a more practical level, the extent to which muscular exertion may be beneficial or detrimental in the treatment of DMD is not known (19). There is no consensus regarding the potential benefits of physical therapy to treat DMD. Thus, it remains unclear whether there is a type and level of exercise that might prove prophylactic for dystrophic muscles, or whether muscle activity and decline are irrevocably linked (20). Answering these questions has direct and immediate implications for the tens of thousands of patients currently enduring DMD (21). Faced with these limitations, a recent roundtable session convened at the New Directions in Biology and Disease of Skeletal Muscle Conference. Several recommendations were agreed on to improve understanding of the role of muscular exertion in the pathology of DMD (20). Chief among these recommendations was the development of new assays and animal models better reflecting the disease in humans. This would permit the use of genetic techniques to understand the pathology of DMD, as well as to identify and evaluate therapeutic approaches.

For decades, the nematode *Caenorhabditis elegans* has been fruitfully used to model human disorders (22). *C. elegans* worms that genetically model DMD through loss-of-function mutations in dystrophin homolog (*dys-1*) are hyperactive and hypercontracted (23). Like DMD patients, *dys-1* mutant worms display muscle weakness, which improves with prednisone and melatonin treatments (24). Under standard growth conditions (crawling on agar plates), *dys-1* mutants display modest muscular and mitochondrial degeneration. However, combining *dys-1* mutations with mutations in other muscle-related proteins (e.g., the ortholog of the myogenic regulatory factor, *hlh-1*) has provided insight into the role of dystrophin in healthy and compromised muscles (25). Many dystrophin-related genes have now been identified in *C. elegans* (including components of the dystrophin glycoprotein complex, acetylcholine transporters, and channels responsible for calcium homeostasis) (26). Gain-of-function mutations in *egl-19* (which encodes the L-type voltage-dependent Ca^{2+} channel responsible for excitation–contraction coupling) are sufficient to induce muscle degeneration. Conversely, RNA interference (RNAi)-mediated silencing of *egl-19* expression in dystrophic worms significantly decreased degeneration (27). Mutations in a large-conductance calcium-activated potassium channel expressed in muscle M lines and sarcomere dense bodies (encoded by *slo-1*) elicit progressive muscle degeneration (26), solidifying the consensus of a calcium-mediated mechanism for muscle degeneration in muscular dystrophy.

To further our understanding of the molecular processes involved in degeneration in DMD, we developed a burrowing assay that permits the modulation of substrate density and the resulting muscular exertion produced by burrowing animals (28). Under this paradigm, animals not only modeled DMD genetically but also recapitulated the chronic motor and muscular decline seen in DMD patients (29). We show that burrowing in dystrophic *C. elegans* recapitulates the early onset and sarcoplasmic calcium dysregulation characteristic of DMD. To evaluate the potential impact of different physical activities on dystrophic musculature, we compared natural behaviors performed by worms with distinct intensities and frequencies of muscular exertion. We report that, consistent with in vitro work in mice, sarcoplasmic calcium increase occurs before onset of other overt muscular phenotypes and that calcium release appears unaltered when calcium clearance is challenged in the muscles of freely behaving dystrophic animals. We further show that calcium clearance and other dystrophic phenotypes were improved by reducing calmodulin expression. By modulating the duration and intensity of exercise treatments, we found that longevity in dystrophic animals is inversely related to muscular exertion, but not the frequency at which the animals performed these activities.

Methods

C. elegans was grown on nematode growth media (NGM) agar plates seeded with the *Escherichia coli* strain OP50 at 20 °C as previously described (30). Information on strains, imaging, calcium measurements, behavioral studies, and molecular biology is in *SI Appendix, Methods*.

Results

Burrowing Dystrophic Worms Recapitulate Many of the Features of DMD. Muscle degeneration and necrosis are characteristics of DMD that we saw recapitulated in dystrophic worms. After burrowing in 6% agar for 5 d, adult dystrophic worms showed several signs of degeneration compared with wild-type (WT) worms (*SI Appendix*, Fig. S1). Transmission EM (TEM) images of midbody musculature displayed loss of sarcomere organization (Fig. 1 *A* and *B*). In addition, dystrophic animals showed an increased proportion of abnormal mitochondria compared with WT animals (76% vs. 8%, $P < 0.001$, χ^2 test, $n = 71$ and 39, respectively; Fig. 1 *C* and *D*). Mitochondria were considered abnormal if they displayed membrane swellings or complete loss of the outer membrane and disorganized or degenerated cristae (31).

Compared with crawling, mitochondrial abnormality was exacerbated in burrowing dystrophic animals (Fig. 1 *E* and *F*). We used mitochondrial fragmentation (32) as an indicator for muscle health in dystrophic animals under crawling or burrowing conditions. Fragmentation was assessed from superresolution fluorescence stacks of midbody musculature in animals that had GFP localized to muscle mitochondria (33) (a kind gift from Hongkyun Kim, The Chicago Medical School at Rosalind Franklin University of Medicine and Science, North Chicago, IL). Significant increases in mitochondrial fragmentation were detected by reduction in their area ($P = 0.048$, Mann–Whitney rank sum test, Fig. 1*G*) and increased circularity index ($P = 0.025$, *t* test, Fig. 1*H*).

One of the earliest diagnostic features of DMD in humans is impaired locomotion (34). Day 1 adult worms of two independently derived dystrophic alleles, *dys-1(eg33)* and *dys-1(cx18)*, showed severe burrowing impairments when burrowing in 3% agar ($P < 0.001$, Holm–Sidak, Fig. 1*I*). Furthermore, *dys-1(eg33)* burrowing dystrophic worms had a reduced life span compared with healthy WT animals ($P < 0.001$, Cox proportional hazard, Fig. 1*J*).

Burrowing dystrophic *C. elegans* worms thus recapitulated some of the most salient phenotypes of the disease in humans. They model DMD genetically and in muscular degeneration, motor deficits, and reduced longevity. In humans, loss-of-function mutations in dystrophin manifest during childhood (35). To determine whether burrowing larval *C. elegans* recapitulated the progression of the disease in humans, we turned next to test developing dystrophic worms.

Developing Dystrophic Animals Show Deficits That Parallel the Disorder in Humans. Recently hatched dystrophic L1 larvae had significantly lower crawling velocities than WT L1 larvae ($P = 0.018$, *t* test, Fig. 2*A*). Cytosolic calcium dysregulation in muscles has been proposed as one possible mechanism responsible for the early decline of dystrophic muscle performance. To measure and compare calcium levels in the musculature of dystrophic and healthy animals, we crossed the dystrophic BZ33 strain [*dys-1 (eg33)*] and the ZW495 strain [*myo-3p::GCamp2 + lin-15(+)*], which expresses the calcium reporter GCaMP2 in body-wall musculature of WT animals under the control of the *myo-3* promoter. The new AVG6 strain expresses GCaMP2 in body-wall muscles of dystrophic [*dys-1(eg33)*] animals. This alteration did not overtly affect the BZ33 phenotype, as crawling velocity for both strains remained similar (0.50 vs. 0.48 cm/min, $P = 0.78$, *t* test, $n > 10$; also see *SI Appendix*, Fig. S2).

As an initial test to assess potential calcium dysregulation in dystrophic muscles during animal development, we compared

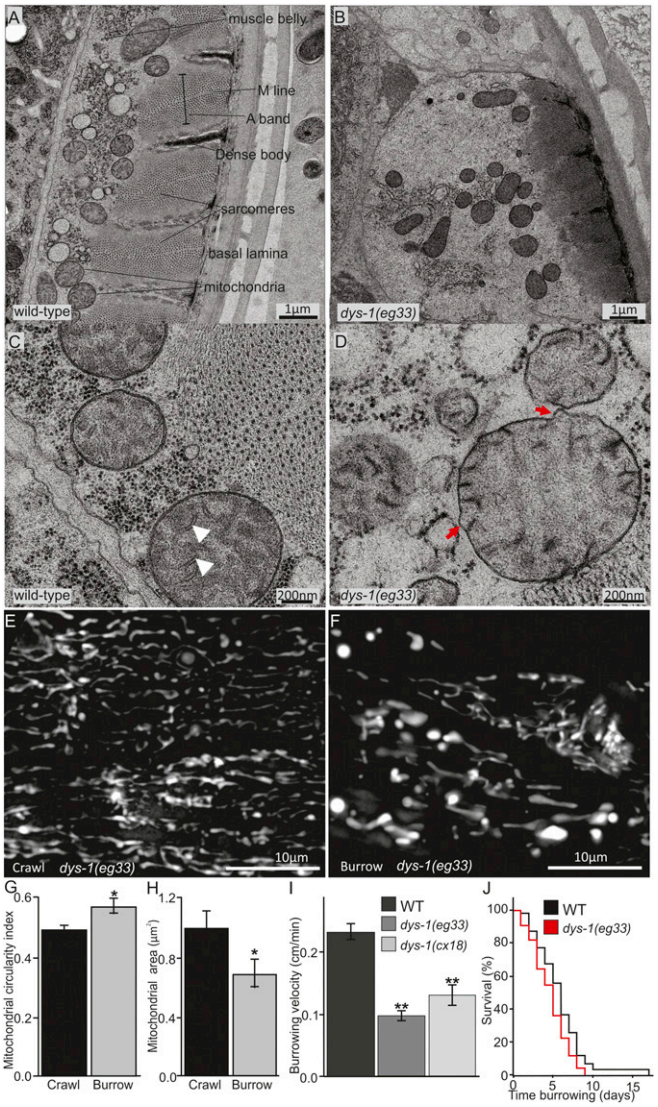

Fig. 1. Burrowing *dys-1* mutants recapitulate cellular, behavioral, and life span phenotypes associated with DMD. (*A–D*) Representative TEM images. (*A*) WT animals that burrowed in 6% agar for 5 d displayed healthy body-wall muscles with well-ordered thin and thick filaments, clear dense bodies, and rounded mitochondria. (*B*) After 5 d, dystrophic animals lost muscle fiber organization, including blebbing mitochondria and rounding of the muscle cells. (*C*) In control burrowing animals, mitochondria displayed clear cristae (white arrowheads) and roundness. (*D*) Dystrophic animals possessed less round mitochondria that displayed signs of membrane degradation (red arrows). (*E* and *F*) Representative 3D structured illumination microscopy superresolution images. (*E*) Fluorescence-tagged mitochondria lines in crawling *dys-1(eg33)* mutants, which maintained clearly visible lines of mitochondria along the muscle fibers. (*F*) Burrowing dystrophic animals displayed blebbing mitochondria lines and increased circularity. On average, mitochondria were more circular (*G*), and smaller (*H*) in burrowing animals. (*I*) *dys-1* mutants carrying independent loss-of-function alleles *eg33* and *cx18* showed decreased burrowing velocity. (*J*) Adult *dys-1(eg33)* worms cultivated in agar showed decreased longevity. Refer to Dataset S1 or results section for comparative and descriptive statistics. $^{**}P < 0.001$, $^{*}P < 0.05$.

the peak GCaMP2 signals of WT and dystrophic L1 larvae. On average, the peak GCaMP2 signal from dystrophic animals was significantly higher than that of WT larvae ($P < 0.001$, Mann–Whitney rank sum test, Fig. 2*B*). This difference was not the result of increased levels of *myo-3* or GCaMP2 expression, as qPCR comparisons in mRNA levels failed to show significant differences between dystrophic and WT strains [*myo-3*: relative quantity (RQ) = 0.85; GCaMP2: RQ = 1.298]. Thus, dystrophic animals appear to suffer muscular damage early on during development, perhaps due to moving in ovo. Differences in crawling velocity and GCaMP2 signals remained significant after animals

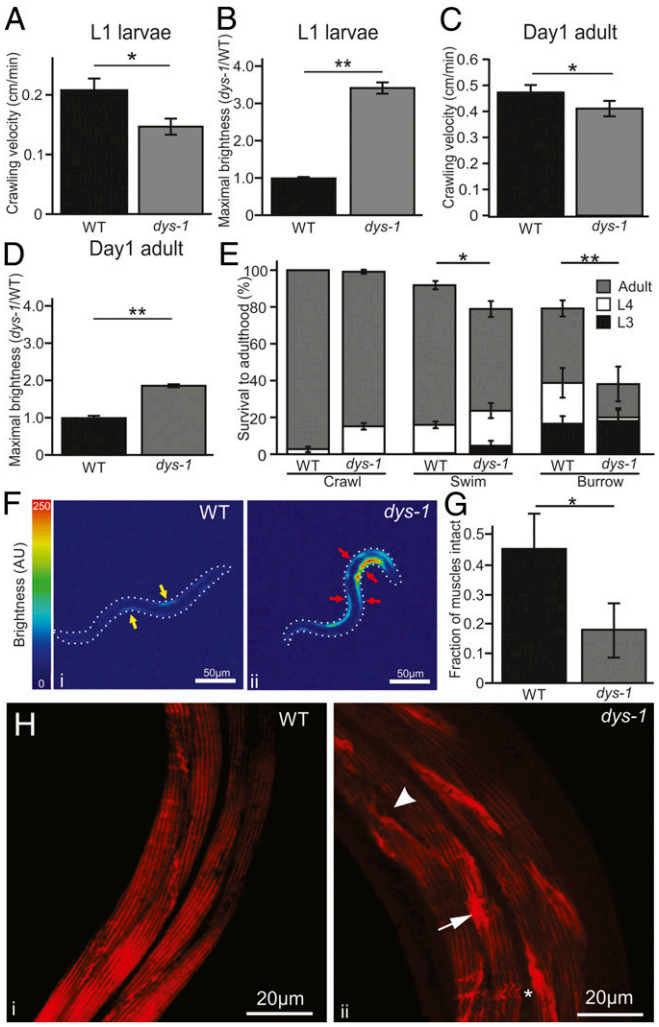

Fig. 2. Dystrophic *C. elegans* displays motor and physiological deficits early in development. (*A*) Recently hatched dystrophic L1 larvae have reduced crawling velocity compared with WT larvae. (*B*) Muscular cytosolic calcium concentration was measured indirectly through GCaMP2 expression in body-wall musculature (driven by the promoter for myosin heavy chain A, *Pmyo-3*). Young dystrophic larvae (L1) were more than three times brighter than WT. Peak (whole animal) brightness normalized to WT is reported. After burrowing to adulthood for 3 d, dystrophic adult animals were still impaired in locomotion (*C*) and increased cytosolic calcium levels (*D*). (*E*) Compared with WT, burrowing *dys-1* larvae showed increased mortality and developmental delays, with roughly half of surviving animals reaching adulthood after 3 d. (*F*) Heat maps showing the relative GCaMP2 brightness of WT (*i*) and dystrophic L1 (*ii*) larvae. AU, arbitrary unit. WT animals had low amplitude signals in the contracting musculature and no detectable signal in relaxed muscles (yellow arrows). Dystrophic larvae displayed brighter GCaMP2 signals, including concomitant activation of antagonistic muscles (red arrows). (*G*) After burrowing to adulthood, less than 20% of dystrophic muscle showed no sign of damage (visualized through phalloidin staining of F-actin) and remained healthy, whereas this count was above 40% in burrowing WT animals. (*H*) Dystrophic animals that survived burrowing to adulthood (*ii*) had signs of muscular degeneration compared with WT animals (*i*), including actin accumulation (arrow), discontinuation of fibers (arrowhead), and wavy muscle fibers (asterisk). $^{**}P < 0.001$, $^{*}P < 0.05$.

burrowed to adulthood (crawl velocity: $P < 0.05$, Mann–Whitney rank sum test, Fig. 2*C*; GCaMP2: $P < 0.001$, *t* test, Fig. 2*D*).

High mortality and developmental delays are associated with DMD (36, 37). To evaluate the effects that differential muscular exertion had on dystrophic larvae, we cultivated L1 worms to adulthood in different exercise regimes: animals either burrowing in 3% NGM agar, swimming in liquid NGM, or crawling on 3% Petri plates. After 3 d (20 °C), we found that surviving dystrophic worms had greater developmental delays than WT worms, regardless of treatment (Fig. 2*E*). In each treatment, more dystrophic animals remained in larval stages compared with WT animals (*t* test for each treatment, $P < 0.01$, Fig. 2*E*). This was most pronounced during burrowing: Only half of surviving dystrophic worms reached adulthood by this time point. Burrowing dystrophic larvae also suffered increased mortality: Only 40% of dystrophic animals were alive after 3 d of cultivation in 3% agar. Similar results were obtained when the agar density was increased to 6% (*SI Appendix*, Fig. S3*C*). In contrast, WT larvae had twice that survival rate (80%).

To generate rhythmic locomotion, antagonistic muscle groups in *C. elegans* contract in alternation. Accordingly, we found that in WT larvae, GCaMP2 activation was restricted to contracting muscles (yellow arrows in Fig. 2 *F*, *i*). However, in dystrophic larvae, GCaMP2 fluorescence was present not just in contracting muscles but also in their antagonists (red arrows in Fig. 2 *F*, *ii*). This increase in noncontracting muscles led to a significant increase in peak brightness of L1 larvae ($P < 0.001$, Mann–Whitney rank sum test, Fig. 2*B*), which continued as the animals grew to adulthood ($P < 0.001$, *t* test, Fig. 2*D*), suggesting either an increase in baseline calcium levels or an inability to timely—and fully—clear sarcoplasmic calcium during the relaxation part of the cycle. Either scenario would require ever-greater calcium transients from contracting muscles to achieve locomotion and could add further strain to dystrophic muscles. Indeed, when we stained F-actin in animals that had burrowed to adulthood, we found that a larger fraction of muscles in WT animals remained undamaged, with no signs of degeneration, as compared with dystrophic animals ($P < 0.05$, χ^2 test, Fig. 2*G*). We defined damage as wavy (detached) filaments, ectopic actin accumulation, or missing filaments (Fig. 2*H*). Dystrophic *C. elegans* thus appears to match the human disease not only in loss of motility, early onset, developmental delays, and high mortality, but also in muscular degeneration.

Dystrophic Worms Display Increased Levels of Sarcoplasmic Calcium. To assess the progression of calcium dysregulation, we tracked calcium changes as animals burrowed in 3% agar over time. Day 1 adults were placed in burrowing wells and evaluated after 1, 3, and 5 d. We used a ratiometric approach to measure changes in sarcoplasmic calcium, using the ratio of contracted to relaxed muscles (see *SI Appendix*, *Methods* for details). We found that WT and dystrophic animals had similar ratios, indicating similar fold changes in sarcoplasmic calcium during contractions. This ratio decreased over time ($P < 0.001$, *t* test, day 1 vs. day 5 each strain), but remained similar between the two strains (Fig. 3*A*). This result was in stark contrast to locomotion velocity, in that day 5 dystrophic animals were significantly slower than WT animals ($P = 0.019$, Mann–Whitney rank sum test, Fig. 3*B*). In an effort to understand the changing relationship between motor output and calcium transients in muscles, we looked closer at the basal and peak levels of sarcoplasmic calcium (i.e., during relaxation and contraction, respectively). We found that in dystrophic animals, peak sarcoplasmic levels of calcium dropped significantly over time for actively contracting muscles ($P = 0.004$, *t* test, Fig. 3*C*), while those for relaxed muscles remained unchanged (Fig. 3*D*). In contrast, peak calcium levels for contracting muscles of WT animals remained unchanged (Fig. 3*D*), but calcium levels for relaxed muscles increased ($P < 0.001$, *t* test, Fig. 3*D*). Changes in calcium levels during the contracted state implicate the release phase of contraction, whereas changes

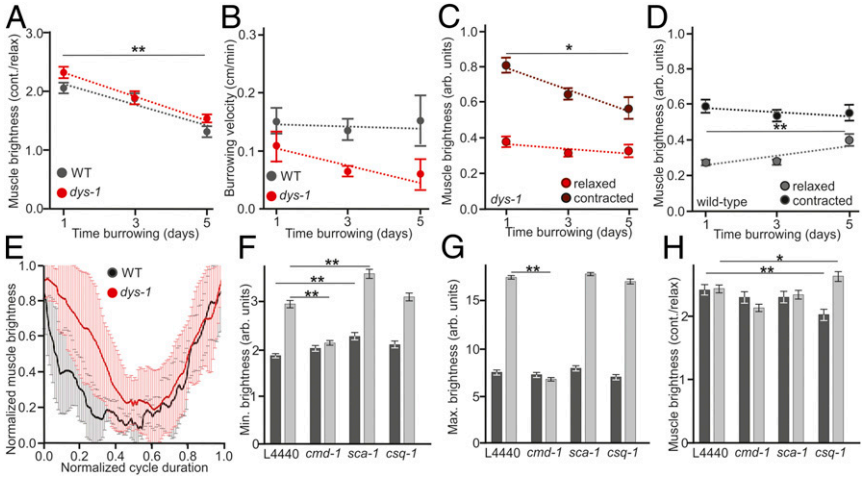

Fig. 3. Calcium release becomes uncoupled from muscle contraction in dystrophic musculature. (*A*) WT and dystrophic worms burrowing continuously in 3% agar over their first 5 d of adulthood. Calcium transients associated with muscular contractions are displayed as the ratio of peak GCaMP2 brightness of contracting to relaxing muscles at the peak of contraction. (*B*) Velocities of WT and dystrophic animals burrowing in 3% agar over time. By day 5, dystrophic animals showed a decline in velocity compared with WT animals. (*C*) Ranges of peak cytosolic calcium muscles over time. (*D*) Dystrophic animals maintained elevated basal levels of cytosolic calcium in relaxed musculature, as well as greater levels in contracting muscles, which decline over time. (*E*) Kinetics of calcium transients during muscle contraction evaluated indirectly through GCaMP2 brightness measurements. Muscle brightness was measured during several (>5) crawling cycles in (>5) WT, and dystrophic animals. Peak brightness is shown normalized to cycle duration, and muscle brightness is normalized to entire brightness range. Dystrophic worms showed delayed and incomplete calcium clearance during the relaxation phase of the cycle (0.0 to 0.5) but showed no difference from WT worms during the contraction phase of the cycle (0.5 to 1.0). We used RNAi to reduce SERCA (*sca-1*) (*F*), calmodulin (*cmd-1*) (*G*), and calsequestrin (*csq-1*) expression (*H*) in WT and dystrophic worms. (*F*) Reducing SERCA expression increased basal calcium levels in both dystrophic and WT animals. (*G*) Reducing calmodulin expression returned dystrophic animals to WT calcium levels for their basal brightness and peak brightness during contraction. (*H*) Reducing calsequestrin significantly affected amplitude of the calcium transient during contractions in distinct manners, increasing the ratio for dystrophic worms and decreasing the ratio for WT worms. $^{**}P < 0.001$, $^{*}P < 0.05$. Dark bars, WT; light bars, *dys-1* animals.

during the relaxed state point to the calcium clearance phase. Although distinct, these changes are consistent with the decline observed in the contracted-to-relaxed brightness ratio measured in Fig. 3*A*.

Higher Basal Levels of Sarcoplasmic Calcium Are Associated with Delays in Clearance, Leading to Incomplete Relaxation. Dysregulation in cytosolic calcium levels has been reported in dystrophic musculature before (38), but are all calcium processes equally susceptible to this insult? During muscle contractions, calcium is initially released from internal stores and becomes free to mediate actomyosin interactions. After contraction, calcium is cleared from the sarcoplasm before the onset of a new contractile event. Although these processes must be tightly coupled in healthy muscles, calcium release and clearance are molecularly independent and distinct. Since our results indicated differences in calcium levels between contracted and relaxed muscles, we investigated whether dystrophic animals were impaired in either process. We quantified the dynamics of calcium cycling during muscular contractions. We filmed and analyzed GCaMP2 signals from the dorsal and ventral muscles behind the pharynx of WT and dystrophic worms (muscles 7 and 8) as they freely crawled on agar plates (Fig. 3*E*). To compare calcium kinetics across animals and strains, we normalized the timing of the calcium changes to the movement cycle [starting at the angular peak for the body segment under consideration (cycle time = 0), progressing through the peak of relaxation (cycle time = 0.5), and returning back to the peak of the next body wave (cycle time = 1)]. We next normalized the data by the range of muscle brightness. These transformations allowed us to compare the timing of calcium changes, minimizing concern for movement velocity and signal amplitude. Comparisons of the cycling of sarcoplasmic calcium between WT and dystrophic animals showed that both strains had similar calcium release kinetics during the contraction phase (Fig. 3*E*, second half of the plot). However, dystrophic worms had significantly faster, but incomplete, calcium clearance during the relaxation phase ($P < 0.001$, multivariate analysis of covariance, first half of plot in Fig. 3*E* and *SI Appendix*, Fig. S2*F*). The incomplete clearance of sarcoplasmic calcium during the relaxation phase of the muscle contractile cycle is consistent with the increased levels of calcium we observed for burrowing dystrophic worms (Fig. 3*C*) and with the increased brightness of both larval and adult dystrophic muscles (Fig. 2 *B* and *D*). These findings also are in agreement with in vitro calcium recordings from dystrophic mice, in which dystrophic muscle fibers were shown to display altered calcium clearance but normal calcium release (39). Our results in freely moving animals illustrate the functional consequences of this impairment for dystrophic muscles.

Contribution of Calcium Handling Genes to Increased Calcium in Dystrophic Musculature. As mentioned above, calcium signaling genes such as *slo-1* and *egl-19* have been implicated in muscle degeneration (26, 27). To further investigate the nature of intracellular calcium movement in WT and dystrophic animals, we used RNAi to either reduce the levels of the cytosolic calcium binding protein calmodulin (CMD-1), SERCA (SCA-1; responsible for moving calcium into the sarcoplasmic reticulum), or calsequestrin (CSQ-1; responsible for calcium buffering within the sarcoplasmic reticulum). RNAi silencing reduces expression levels of genes whose knockout would be lethal and is a well-established technique in *C. elegans* (40). Upon silencing different calcium handling genes, we identified three distinct effects: (*i*) silencing the worm homolog of SERCA (*sca-1*) selectively increased basal calcium levels as measured by the basal brightness in both dystrophic and WT animals ($P < 0.001$ and $P = 0.009$, respectively, *t* test, Fig. 3*F*); (*ii*) surprisingly, silencing calmodulin reduced the basal and peak brightness of dystrophic muscles down to WT levels but had no effect on WT animals (minimum $P < 0.001$, maximum $P = 0.01$, *t* test, Fig. 3 *F* and *G*); however, silencing calmodulin did not significantly affect the calcium transients produced during muscle contraction (as measured by the ratio of contracted-to-relaxed fluorescence) (Fig. 3H); and (*iii*) consistent with its proposed role in helping regulate calcium release during contraction (but not clearance during relaxation), silencing calsequestrin selectively affected the contracted-to-relaxed brightness ratio in both WT and dystrophic animals, albeit in different directions ($P < 0.001$ and $P = 0.048$, respectively, *t* test, Fig. 3*H*).

Reducing Calmodulin Expression Improves Function in the Dystrophic Muscles of Worms. The finding that reducing calmodulin expression in dystrophic muscles reduced calcium to WT levels (as measured by GCaMP2) was unexpected. Previous evidence from work in mice suggested that targeted inhibition of calmodulin exacerbates the dystrophic phenotype in these animals (41). After verifying calmodulin silencing in RNAi-treated animals through qPCR, we further characterized the effect of reducing *cmd-1* expression in dystrophic animals (Fig. 4). Although silencing *cmd-1* in *dys-1(eg33)* animals had no significant effect on their crawling velocity (Fig. 4*A*), comparison of their calcium dynamics during contraction and relaxation cycles showed that the calcium clearance phase of the cycle (first half) was dramatically improved in comparison with dystrophic animals that were fed the empty RNAi vector (L4440, Fig. 4*B*). Calcium levels during relaxation of the muscles thus dropped faster, reducing the remaining basal calcium levels. To test whether this also improved the impaired burrowing ability of dystrophic worms, we tested *cmd-1*–silenced worms in a burrowing race assay. Briefly,

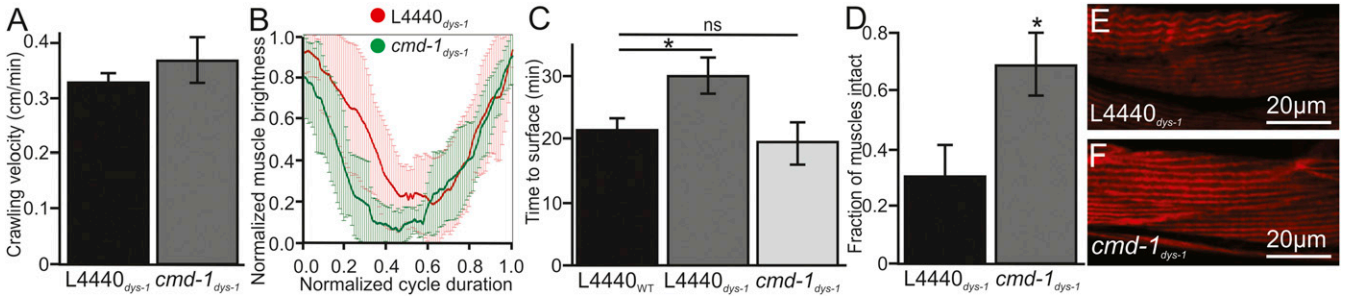

Fig. 4. Reducing calmodulin expression helps alleviate the dystrophic phenotype in *C. elegans* modeling DMD (*A*). RNAi silencing of calmodulin had no effect on the crawling velocity of *dys-1* worms. (*B*) Kinetics of calcium transients for dystrophic worms fed empty RNAi vectors (L4440) or RNAi targeting calmodulin (*cmd-1*). (*C*) *cmd-1* RNAi-treated animals burrowed faster than WT animals to an attractant on the surface of a burrowing well. (*D*) Compared with RNAi control (L4440), calmodulin-silenced dystrophic animals had a greater fraction of healthy muscles. (*E* and *F*) Dystrophic day 1 adults displayed wavy actin fibers near the midbody (*E*), whereas the calmodulin-silenced worms had limited actin accumulation or signs of other fiber degeneration (*F*). ns, nonsignificant. *$P < 0.05$.

animals were placed at the center of a 3-mL 6% NGM agar volume, and the time they required to burrow to an attractant placed at the surface of the well was compared with control dystrophic and WT animals (Fig. 4*C*). We found that silencing *cmd-1* in *dys-1(eg33)* animals restored their burrowing ability back to WT levels in this assay ($P = 0.607$ vs. WT control, *t* test, Fig. 4*C*). Furthermore, quantification of muscle health showed a significant increase in the number of intact muscle fibers compared with control dystrophic animals fed bacteria containing the control L4440 vector ($P = 0.035$, χ^2 test, Fig. 4 *D–F*). Work on human dystrophic muscles revealed elevated calmodulin levels in DMD muscles compared with other primary myopathies and age-matched controls (particularly in the early stages or in mildly progressive stages) (42). While it is beyond the scope of this work to fully discern the role of calmodulin in the progression of muscular dystrophy, it is clear that it plays a complex and important role in this disease (43, 44).

Locomotion Through Different Physical Environments Places Distinct Demands on the Musculature of *C. elegans*. The extent to which muscle decline is precipitated by either impaired calcium trafficking or by mechanical damage from its contractile machinery has important implications for the type of muscle (and activities) that might be most susceptible to injury and/or treatment in dystrophic patients. If the contractile machinery is largely responsible for the observed muscle decline, it might be possible to recruit the muscular repair response by means of low-intensity, high-frequency exercise (e.g., swimming) without compromising muscle integrity in the process. However, if calcium dysregulation plays an important role in the pathology of DMD, high-frequency exercise might further challenge compromised calcium release and clearance machineries, overwhelming the dystrophic muscle and causing more damage. Evidence from different studies has been inconclusive (45). To evaluate the potential benefit of differential muscle activation in dystrophic muscles, we harnessed the natural behavioral repertoire of worms. *C. elegans* crawls on solid surfaces, swims in liquids, and burrows through dense media (29, 46, 47). During these types of locomotion, the worms adopt distinct body shapes (Fig. 5*A*) and locomotion kinematics. We found that swimming was the fastest of the three behaviors, with the highest body-bend frequencies and the lowest bending amplitudes (velocity: $P < 0.001$, Kruskal–Wallis ANOVA on ranks, Fig. 5 *B* and *C*). Crawling had an intermediate average velocity, with larger bending amplitudes and intermediate frequencies. Burrowing was the slowest of the three behaviors and had the lowest frequencies and greatest bending amplitudes (burrow velocity vs. swim and crawl: $P < 0.001$, Kruskal–Wallis ANOVA on ranks; burrow vs. swim: $P < 0.05$, Dunn's post hoc test at $P < 0.05$; Fig. 5). This is consistent with previous force output estimates increasing from swimming [1 to 3 μN (48)] to crawling [5 μN (49)] to burrowing [19 to 31 μN (50)]. Exertion by burrowing worms can be modulated by varying the density of the media (29). The anterior end of worms houses a greater number of muscles compared with medial or posterior regions of similar length. Not surprisingly, we found that the head of *C. elegans* appears to contribute to propulsion disproportionately compared with the rest of its body, undergoing the greatest angular excursion during all types of locomotion ($P < 0.001$, one-way ANOVA, Fig. 5*D*). This asymmetry was reduced for burrowing animals, in which the posterior musculature appeared to be recruited more equitably to achieve locomotion ($P = 0.012$, one-way ANOVA, Fig. 5*E*).

To determine whether the different kinematics observed within body regions and between behaviors correlated with muscular exertion, we filmed animals expressing GCaMP2 in their musculature. Paralleling our kinematic measurements, burrowing animals displayed the strongest change in brightness ($P < 0.001$, one-way ANOVA, Fig. 5*G*). While still displaying posterior dampening, burrowing animals produced the greatest calcium transients across their entire bodies. In contrast, the musculature of swimming worms produced low calcium transients similar in amplitude across the length of their bodies. Therefore, swimming by *C. elegans* requires fast and shallow movements across the whole body that do not require great muscular output. In contrast, burrowing consists of slow, deep-body contractions that require powerful output from the animal's musculature. We conclude that these locomotor modalities can mimic regimens involving high-frequency, low-intensity (swimming), or high-intensity, low-frequency (burrowing) activity.

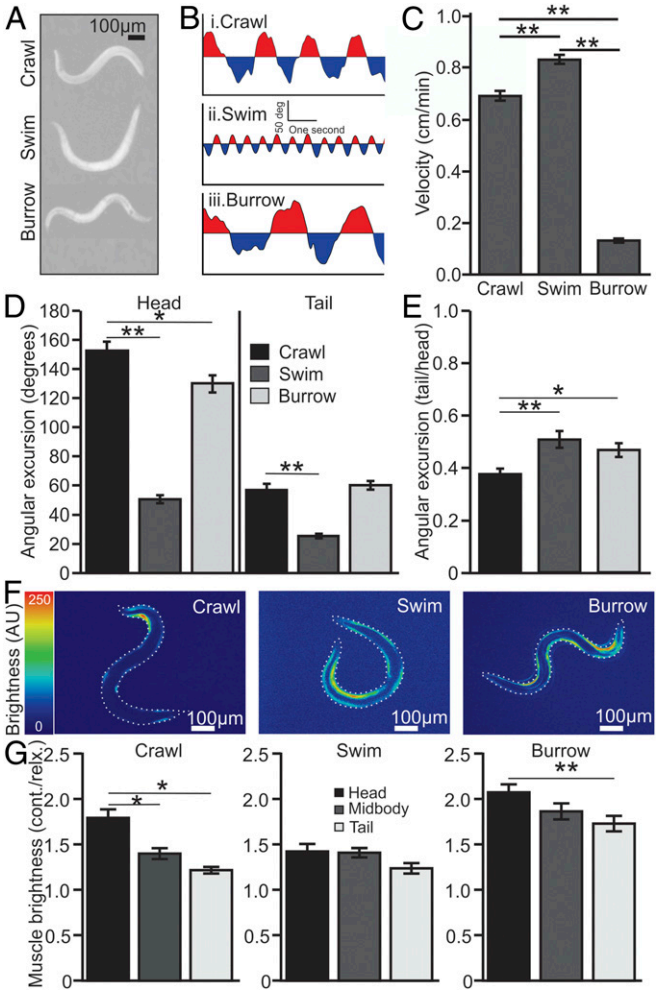

Fig. 5. Locomotion through different environments is associated with distinct muscle output in *C. elegans* (*A*). Representative images of *C. elegans* crawling on solid surfaces, swimming in liquid, and burrowing through media, adopting characteristic "S," "C," and "W" shapes, respectively. (*B*) Neck curvature plots for crawling, swimming, and burrowing worms illustrating that burrowing consists of low-frequency, high-amplitude movements, whereas swimming relies on high-frequency, low-amplitude movements. (*C*) Each behavior has characteristic velocity ranges. (*D*) Movement amplitudes differ between behaviors and across the length of the animals. Animals crawled using large head flexions that did not propagate fully to their tail. (*E*) The contribution of the tail muscles to locomotion was greater during swimming and burrowing than during crawling. (*F*) The anterior bias in propulsion for all behaviors, as well as the increasing contribution of posterior musculature during swimming and burrowing, is reflected by muscular calcium transients. Heat maps show variations in cytosolic calcium in body-wall musculature inferred from GCaMP2 fluorescence (driven by the *myo-3* promoter). (*G*) Quantification of calcium transients for different areas of the body during crawling, swimming, and burrowing. Although slower, burrowing produced the greatest calcium transients across the entire body of the worm. $^{**}P < 0.001$, $^{*}P < 0.05$.

Dystrophic Muscles Do Not Benefit from Increased Frequency or Intensity of Contraction. Next, we set out to determine whether changes in the motor demands have the potential to delay or prevent some of the phenotypes associated with muscular dystrophy. We placed dystrophic day 1 adult worms to either crawl on agar plates, burrow in 3% agar wells, or swim in liquid NGM. We measured their locomotion velocities and calcium transients after 1, 3, and 5 d of treatment. As shown in Fig. 6 *A* and *B* (see *SI Appendix*, Fig. S4 for WT), swimming worms experienced a loss in velocity between days 1 and 5 ($P = 0.003$, Mann–Whitney rank sum test) while displaying an increase in the brightness ratio of relaxed to contracted muscles ($P < 0.05$, Mann–Whitney rank sum test). These data suggest that swimming dystrophic animals are unable to maintain normal propulsion despite ever-greater calcium transients. Burrowing worms displayed a decline in calcium transients ($P < 0.001$, *t* test, Fig. 6 *A* and *B*). Crawling animals maintained their velocity throughout the experimental period, but, similar to swimming animals, calcium transients increased significantly by day 5 ($P < 0.001$, *t* test, Fig. 6*B*). One potential explanation for these data is that as the musculature of dystrophic animals degenerates, propulsive forces decrease. This may then be compensated by an increase in calcium release during contraction to achieve greater recruitment of the remaining pool of intact actomyosin fibers (resulting in an increased contraction-to-relaxation brightness index). In contrast to crawling and swimming, burrowing animals might already start challenged and thus only show a continuous decrease in their contraction-to-relaxation brightness ratio.

By the end of the burrowing treatment (day 5), only about 50% of the animals were still alive (Fig. 6*C*). Burrowing animals had significantly decreased longevity compared with crawling ($P < 0.001$, Cox proportional hazard) and swimming animals ($P < 0.001$, Cox proportional hazard), while there was no difference between crawling and swimming animals ($P = 0.354$, Cox proportional hazard). This is consistent with only minor longevity increments recently reported for WT animals under short-duration swimming treatments (and food deprivation) (51). Confocal images of the body-wall musculature after treatment showed that although the F-actin fibers of crawling and swimming worms were mostly intact, 57% of burrowing animals (vs. 12% of crawling animals, $P = 0.012$, χ^2 test, Fig. 6*D*) displayed signs of damage.

While neither activity increased longevity or muscle health, burrowing had a clear negative effect on every metric considered. It is possible, however, that the continuous burrowing overwhelms the coping ability of dystrophic muscles, whereas a more limited treatment might produce beneficial effects. A recent study by Laranjeiro et al. (52) subjected worms to 90 min of swimming per day and showed that this was sufficient to induce many of the molecular hallmarks of exercise. To evaluate the effect of shorter-duration treatments, we repeated the experiments above but restricted their duration to 90 min/d.

Altering Exercise Duration Affected Several Muscular Parameters but Not Animal Longevity. Dystrophic animals swimming 90 min/d had a reduced drop in swimming velocity compared with worms continuously swimming ($P < 0.001$, Kruskal–Wallis one-way ANOVA on ranks, Fig. 7*A*). However, calcium transients continued to increase in both treatment groups over the 5 d of the experiment (continuous swimming: <0.05, Tukey's test; intermittent burrowing: <0.05, Dunn's method; Fig. 7*B*). Mirroring the effects of intermittent swimming, worms that burrowed only 90 min/d showed greater velocity compared with those that burrowed continuously ($P < 001$, *t* test, Fig. 7*C*). However, the greatest differences between continuous and intermittently burrowing worms were observed at the beginning of the treatment, declining thereafter ($P < 0.001$, one-way ANOVA, Fig. 7 *C* and *D*).

To further evaluate the effect of burrowing duration on dystrophic muscles, we imaged F-actin fibers. We found that animals burrowing only 90 min/d had significantly larger muscle cells than worms that burrowed continuously (Fig. 7*F* and *SI Appendix*, Fig. S5). This effect was even greater for healthy WT worms (WT $P < 0.001$, dystrophic $P < 0.05$, *t* test, Fig. 7*F*). Although muscle growth was more marked for midbody muscles, the combined area of the muscles comprising a body quadrant was significant larger in healthy and dystrophic animals that burrowed 90 min daily compared with animals that crawled during the same period (WT $P = 0.004$, dystrophic $P < 0.001$, *t* test, Fig. 7*G*, *Left*). Muscle hypertrophy refers to exercise-mediated muscle growth brought about by increases in the contractile machinery (contractile hypertrophy) or in noncontractile elements (sarcoplasmic hypertrophy) (43, 53). To investigate whether the increase in muscle size was the product of changes in sarcomere diameter, we measured myofibril cross-sectional areas from our confocal stacks of midbody musculature. Consistent with hypertrophy work on mice, we found that WT animals that burrowed intermittently had a significant increase in myofibril

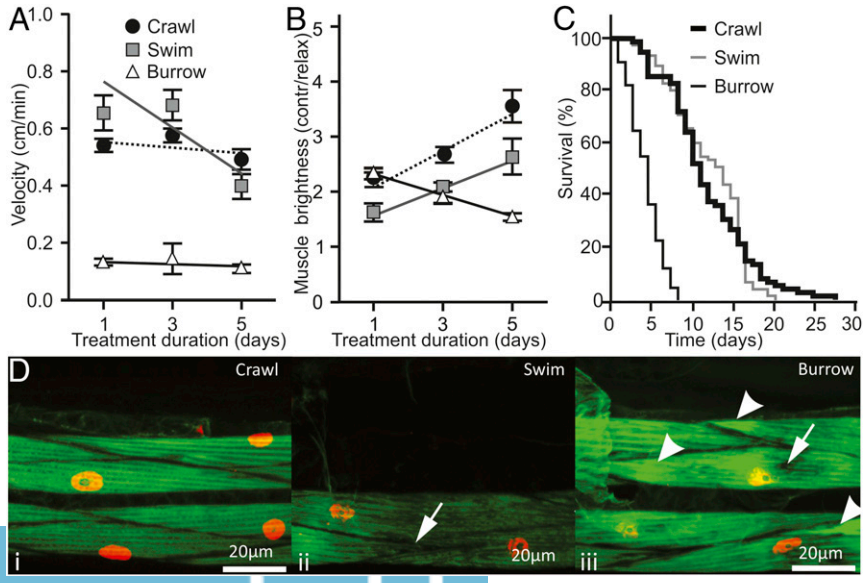

Fig. 6. Physical exertion negatively impacted health and longevity in dystrophic *C. elegans* worms. (*A*) The velocity of burrowing animals declined continuously throughout the experiment, whereas velocities were maintained under swimming or crawling treatments until day 3. (*B*) The decline seen by day 5 in crawling and swimming animals was accompanied by an increase in calcium transients. (*C*) Although swimming and crawling differed in velocity and in calcium transient amplitudes, both activities had similar effects on dystrophic worm longevity. However, burrowing decreased animal longevity significantly compared with other treatments. (*D*) Representative confocal images of dystrophic muscles with phalloidin-stained F-actin after crawling (*i*), swimming (*ii*), or burrowing (*iii*) for 5 d. Swimming and burrowing animals had signs of muscle degeneration, including torn or fewer actin fibers in swimming animals (arrows) and F-actin accumulation at the sides of the muscle cells of burrowing animals (arrowheads). Green is phalloidin-stained F-actin; red is GFP localized to muscle nuclei.

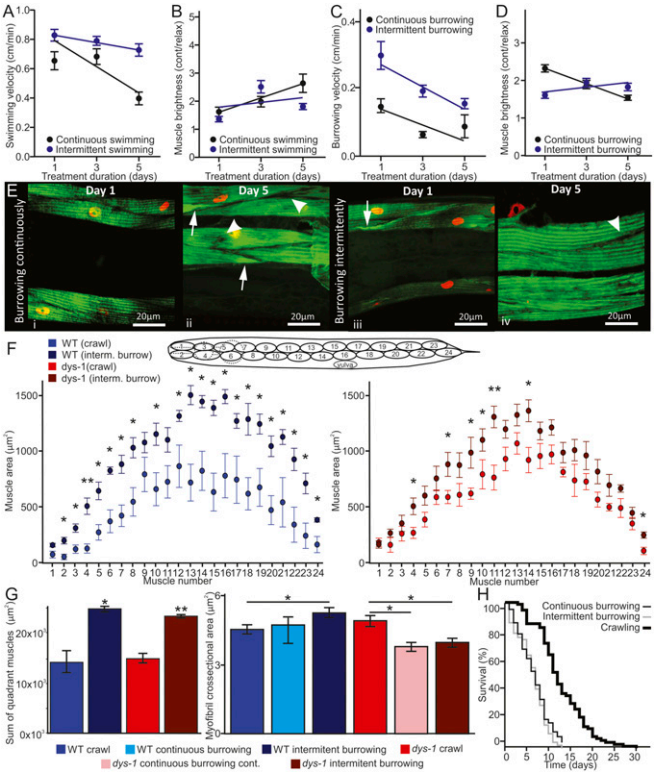

Fig. 7. Intermittent exercise significantly improved some dystrophic muscle metrics, without affecting animal longevity. (*A*) Dystrophic animals that swam only 90 min daily displayed a modest decrease in velocity over time. Continuously swimming animals had a significant drop in swimming velocity. (*B*) The amplitude of calcium transients in dystrophic animals increased significantly over time. (*C*) Worms that burrowed for 90 min daily had the greatest velocity after one exercise session (day 1). However, this effect disappeared over time. (*D*) Animals that burrowed continuously showed a decline in the amplitude of cytosolic calcium transients during locomotion, while animals that burrowed intermittently had a significant increase in these transients. (*E*) Worms that had burrowed continuously for 5 d (*ii*) showed signs of degeneration (arrowheads) as well as actin buildup (arrows). Intermittent-burrowing animals displayed these signs to a lesser extent. (*F*) After 5 d, animals that had burrowed intermittently showed increased cell area compared with animals that crawled continuously in both *dys-1* and WT strains. (*G*) The combined muscle area of all muscle cells in a quadrant in intermittently burrowing animals was greater than that of continuously crawling animals (WT and dystrophic animals). WT animals had a greater myofibril cross-sectional area than crawling controls. However, intermittently burrowing dystrophic worms showed a decrease in myofibril cross-sectional area. (*H*) Animals that burrowed intermittently showed no improvement in longevity. $^{**}P < 0.001$, $^{*}P < 0.05$.

cross-sectional area ($P < 0.05$, *t* test, Fig. 7*G*, *Right*) (54). However, dystrophic animals that burrowed either continuously or 90 min daily showed a significant decrease in myofibril cross-sectional area compared with crawling animals ($P < 0.05$, *t* test, Fig. 7*G*, *Right*). This difference is consistent with the sarcomere areas visible on TEM images (compare Fig. 1*A* with Fig. 1*B*). Furthermore, we found that improvements in velocity and cell growth did not translate to increased longevity for animals that burrowed 90 min daily (compared with those in the continuously burrowing treatment group, Fig. 7*H*). Similar effects were measured for swimming animals (*SI Appendix*, Fig. S3), which indicated that improvements in muscle size and output did not translate into improvements in animal longevity.

Discussion

Modeling DMD with Nematodes. The understanding of the molecular mechanisms responsible for muscle degeneration and death in DMD has benefited from many animal models, ranging from mice to dogs, zebrafish, flies, and worms (12). Each system has intrinsic advantages and limitations, explaining their continued ability to contribute to the understanding of this disorder. One limitation plaguing many models of DMD is the lack of severity of the disorder. Therefore, most studies have resorted to a combinatorial approach combining dystrophin loss with loss in an associated protein or with other types of sensitization (8, 27, 55). While useful, the nature of these approaches complicates interpretation of their findings and draws attention to the obvious question of why humans show such a severe phenotype compared with other animals. These limitations coalesced during the roundtable session convened at the New Directions in Biology and Disease of Skeletal Muscle Conference (20). Several recommendations to improve understanding were later formalized in the 2015 Action Plan for the Muscular Dystrophies developed by the NIH and the Muscular Dystrophy Coordinating Committee (56). To answer the stated needs, we developed an assay in *C. elegans* to investigate the pathology of DMD and identify promising strategies for its treatment. In our burrowing assay, dystrophic worms displayed many of the phenotypes associated with DMD in humans (29). These included increased cytosolic calcium, early onset, loss of mobility, mitochondrial damage, contractile machinery failure, muscle death, and shortened life span. This work complements recent studies with dystrophic worms demonstrating muscle weakness that is improved by drug treatments currently used to treat the disease (24), consolidating *C. elegans* as one of the most complete DMD animal models.

Impaired Clearance of Cytosolic Calcium Is Associated with Increase in Basal Calcium Levels and with Increased Calcium Release During Muscle Contractions. We found that muscles in recently hatched L1 dystrophic larvae had increased levels of calcium compared with WT animals (Fig. 2 *B* and *C*). These findings are consistent with higher cytosolic calcium levels being a hallmark of the early stages of DMD and with calcium's role in mediating muscle degeneration (4, 57). However, when increased basal levels of cytosolic calcium arise, they remain high throughout the life of the dystrophic animal (Fig. 3*D*). In contrast, WT animals see their basal calcium increase to dystrophic levels only by the fifth day of burrowing. Increased basal levels of calcium could result in muscles being in a continuous state of contraction, as calcium would remain in the cytosol to activate the contractile machinery. This inappropriate baseline tension would create the conditions for a double insult on dystrophic muscles. First, it would increase the work required for the appropriately contracting (antagonistic) muscles during their normal activation to achieve locomotion. Second, it would create an environment in which the relaxed muscle would experience forces consistent with eccentric contractions, which are known to induce myofibrilar dysfunction in dystrophic muscles (58). Burrowing dystrophic worms increased their calcium transients enough to produce the same ratio of contracted to relaxed muscle measured in WT animals. Maintaining this ratio appeared necessary to maintain velocity, as animals lost mobility when this ratio dropped. We found that loss of mobility was associated with a decrease in calcium release during contraction for dystrophic animals and with an increase in basal calcium levels in aging WT animals.

Because dystrophic animals seem able to (at least initially) modulate calcium release and maintain muscular output, calcium dysregulation does not seem to be the consequence of a global collapse in calcium cycling. Supporting this idea, we found that the kinetics of calcium release during contraction remained mostly unaffected in dystrophic animals. However, this was not the case for calcium clearance during the relaxation phase of contraction. Calcium clearance was accelerated in dystrophic animals (*SI Appendix*, Fig. S2*F*, first half of plot). However,

perhaps due to a greater amount of calcium present in the cytosol, this increased rate of clearance did not translate into complete calcium clearance before the beginning of the next contraction. This calcium accumulation would result in a continuously increasing muscle tone with reduced force intensity and increasing levels of cocontractions between antagonizing muscles, all of which reduce animal motility and likely contribute to the hypercontracted phenotype characteristic of these animals. In vitro work on mice models of muscular dystrophy also reported calcium increases due to changes in calcium clearance (but not release) associated with an up-regulation in the expression of genes involved in calcium clearance into the sarcoplasmic reticulum, including SERCA1 and 2 (39).

Calmodulin levels were found to be increased in the cytosol, plasmalemma, and sarcoplasmic reticulum of Duchenne patients [compared with tissues of other primary myopathies and healthy controls (42)]. We found that silencing calmodulin expression in dystrophic worms rescued altered calcium levels and kinetics, as well as motor output and muscle degeneration (Fig. 4). Reflecting its ubiquitousness in cellular processes, the role of calmodulin in muscular dystrophy appears to be complex. For example, the greatest increase in intracellular levels of calmodulin was reported during the initial stages of the disease or in mildly progressive cases (42). In addition, in mdx mice (which display mild degeneration), targeted inhibition of calmodulin signaling exacerbates the dystrophic phenotype (41). It thus remains unanswered whether calmodulin plays a single role during the progression of muscular dystrophy and whether its up-regulation is a harmful consequence or an early response to calcium dysregulation. Understanding the mechanism by which basal cytosolic calcium increases in dystrophic musculature remains of paramount importance, because restoring normal calcium levels without compromising the integrity of cellular organelles could remove one of the factors contributing to the accelerated decline of dystrophic musculature.

Harnessing Natural Behaviors to Study the Role of Exertion in Dystrophic Muscle Health. One of the important aspects of DMD that remains unanswered is the extent to which muscular exertion might be beneficial or detrimental in the treatment of DMD (19). To address this need, we used the natural behaviors performed by worms and evaluated their differential loads on the muscular system. Worms crawl on surfaces, swim through liquids, and burrow through solid media (29, 46, 47). Crawling consists of high-amplitude body movements of intermediate frequency (~0.5 Hz). *C. elegans* crawls using mostly the (more numerous) anterior muscles, which requires less force output than burrowing (48–50) and occurs at lower frequencies than swimming. In contrast, swimming is a fast behavior (~2 Hz) and consists of high-frequency, low-intensity body bends (29). Recent work demonstrated that a single swimming bout in *C. elegans* can induce key features reminiscent of exercise in mammals (52). Similarly, our results suggest that burrowing might be able to induce muscle hypertrophy, at least in healthy animals. In their natural habitat, *C. elegans* worms likely spend most of their time burrowing through solid decaying plant matter or soil. Burrowing consists of slow, low-frequency movements of high intensity (29). Comparing these three locomotor strategies in worms allows testing the effects of activities of high frequency and low intensity (i.e., swimming), and high intensity and low frequency (i.e., burrowing). Furthermore, by varying the density of the burrowing media, it is possible to modulate the force required to achieve locomotion (13). Our calcium measurements from animals moving freely through these media support the idea that burrowing requires the greatest muscular exertion, because contracting muscles were twice as bright as antagonistic (relaxing) muscles; in contrast, swimming and crawling required contractions only about 50% brighter than the relaxing baseline (Fig. 5 *F* and *G*).

Dystrophic Animals Required Progressively Greater Calcium Transients to Maintain Motor Output. Over time, even in swimming and crawling dystrophic worms, the amplitude of calcium transients increased, despite the fact that locomotion velocity was maintained. This supports the idea that as dystrophic damage takes its toll on the musculature, greater effort is required to achieve propulsion. Paradoxically, this greater effort could result in further damage to the muscles, creating a runaway effect as calcium transients eventually become uncoupled from motor output. Indeed, by day 5, both crawling and swimming worms showed increases in calcium transients and loss in propulsion (Fig. 6 *A* and *B*). The ability to modulate calcium release to offset ongoing damage was limited and depended on the magnitude of the task. For example, burrowing worms started with large calcium transients, which quickly decreased in amplitude as the musculature became compromised. Swimming had no effect on longevity for either dystrophic or healthy animals. However, a recent study found modest but significant increases in longevity in WT worms by coupling swimming with food deprivation (51). Unlike swimming or crawling, burrowing had profound negative effects on longevity and muscle integrity.

Longevity of Dystrophic Animals Is Determined by the Intensity of the Exercise Performed. We reasoned that reducing the time animals spent in each exercise treatment might improve their prognosis. We found this not to be the case. Swimming and burrowing produced muscle changes consistent with exercise and showed characteristics of resistive training in humans (53). However, neither activity improved the health of dystrophic muscles or animal longevity. Consistent with results on swimming by Laranjeiro et al. (52), we recommend that swimming and burrowing by *C. elegans* might be investigated for their ability to mimic endurance and resistance exercise, respectively. Our results suggest that endurance and strength exercise treatments have the potential to improve some muscle metrics such as muscle size and output, while also hastening muscle fiber degeneration and reducing longevity. The contractile apparatus of dystrophic animals (a primary target of exercise treatments) is not necessarily tied to the fate of the cell (or the animal). In our experiments, reducing calmodulin expression had a beneficial effect on dystrophic musculature.

Much work remains to be done to understand how loss of the dystrophin protein leads to loss of muscle and premature death. Great efforts are currently underway to harness gene or transcription editing, with the goal of restoring dystrophin levels in muscles. While important and promising, these treatments will have limited applicability to the tens of thousands of patients suffering with this disease today. Therefore, complementary to those efforts, it is important to devise ways to improve the health of those currently suffering with DMD. This will require understanding the pathology of the disorder and devising treatments that improve quality of life without compromising life expectancy.

ACKNOWLEDGMENTS. We thank Drs. Hongkyun Kim and Jon Pierce for strains; Dr. Alysia Mortimer for confocal assistance; Ursula Reuter-Carlson and Scott Robinson for assistance with TEM; Wai Pang Chan and the Biology Imaging Facility at the University of Washington; Alison North at The Rockefeller University; and Marguerite Vantangoli Policelli at GE Healthcare Life Sciences for help on 3D structured illumination microscopy. Chance Bainbridge, Yazmine Giliana, Sruthi Singaraju, and Lavanya Sathyamurthy contributed to experiments. Some strains were provided by the Caenorhabditis Genetics Center (funded by NIH Grant P40 OD010440). Funding was provided by NIH Grants 1R15AR068583-01A1 (to A.G.V.-G.), R01GM111566 (to N.E.S.), and 5T32NS099578 (to S.R.); an Illinois State University Startup funds and University Research Grant Award (A.G.V.-G.); and the Simons Foundation/Simons Foundation Autism Research Initiative Grant 488574 (to A. Singhvi).

1. Goldstein JA, McNally EM (2010) Mechanisms of muscle weakness in muscular dystrophy. *J Gen Physiol* 136:29–34.
2. Hoffman EP, Brown RH, Jr, Kunkel LM (1987) Dystrophin: The protein product of the Duchenne muscular dystrophy locus. *Cell* 51:919–928.
3. Le Rumeur E, Winder SJ, Hubert JF (2010) Dystrophin: More than just the sum of its parts. *Biochim Biophys Acta* 1804:1713–1722.
4. Duncan CJ (1978) Role of intracellular calcium in promoting muscle damage: A strategy for controlling the dystrophic condition. *Experientia* 34:1531–1535.
5. Vila MC, et al. (2017) Mitochondria mediate cell membrane repair and contribute to Duchenne muscular dystrophy. *Cell Death Differ* 24:330–342.
6. Ohlendieck K (2000) The pathophysiological role of impaired calcium handling in muscular dystrophy. *Madame Curie Bioscience Database* [Internet] (Landes Bioscience, Austin, TX). Available at https://www.ncbi.nlm.nih.gov/books/NBK6173/. Accessed March 1, 2018.
7. Smith BF, et al. (2011) An intronic LINE-1 element insertion in the dystrophin gene aborts dystrophin expression and results in Duchenne-like muscular dystrophy in the corgi breed. *Lab Invest* 91:216–231.
8. Kucherenko MM, et al. (2008) Genetic modifier screens reveal new components that interact with the Drosophila dystroglycan-dystrophin complex. *PLoS One* 3:e2418.
9. Giugia J, Gieseler K, Arpagaus M, Ségalat L (1999) Mutations in the dystrophin-like dys-1 gene of Caenorhabditis elegans result in reduced acetylcholinesterase activity. *FEBS Lett* 463:270–272.
10. Tanabe Y, Esaki K, Nomura T (1986) Skeletal muscle pathology in X chromosome-linked muscular dystrophy (mdx) mouse. *Acta Neuropathol* 69:91–95.
11. Gieseler K, Grisoni K, Ségalat L (2000) Genetic suppression of phenotypes arising from mutations in dystrophin-related genes in Caenorhabditis elegans. *Curr Biol* 10: 1092–1097.
12. McGreevy JW, Hakim CH, McIntosh MA, Duan D (2015) Animal models of Duchenne muscular dystrophy: From basic mechanisms to gene therapy. *Dis Model Mech* 8: 195–213.
13. Hirst RC, McCullagh KJ, Davies KE (2005) Utrophin upregulation in Duchenne muscular dystrophy. *Acta Myol* 24:209–216.
14. Petrof BJ, Shrager JB, Stedman HH, Kelly AM, Sweeney HL (1993) Dystrophin protects the sarcolemma from stresses developed during muscle contraction. *Proc Natl Acad Sci USA* 90:3710–3714.
15. Takagi A, Kojima S, Ida M, Araki M (1992) Increased leakage of calcium ion from the sarcoplasmic reticulum of the mdx mouse. *J Neurol Sci* 110:160–164.
16. Khairallah RJ, et al. (2012) Microtubules underlie dysfunction in Duchenne muscular dystrophy. *Sci Signal* 5:ra56.
17. Young CN, et al. (2012) P2X7 purinoceptor alterations in dystrophic mdx mouse muscles: Relationship to pathology and potential target for treatment. *J Cell Mol Med* 16:1026–1037.
18. Gervásio OL, Whitehead NP, Yeung EW, Phillips WD, Allen DG (2008) TRPC1 binds to caveolin-3 and is regulated by Src kinase–Role in Duchenne muscular dystrophy. *J Cell Sci* 121:2246–2255.
19. Engel JM, Kartin D, Carter GT, Jensen MP, Jaffe KM (2009) Pain in youths with neuromuscular disease. *Am J Hosp Palliat Care* 26:405–412.
20. Markert CD, Case LE, Carter GT, Furlong PA, Grange RW (2012) Exercise and Duchenne muscular dystrophy: Where we have been and where we need to go. *Muscle Nerve* 45:746–751.
21. Gianola S, et al. (2013) Efficacy of muscle exercise in patients with muscular dystrophy: A systematic review showing a missed opportunity to improve outcomes. *PLoS One* 8: e65414.
22. Sleigh J, Sattelle D (2010) C. elegans models of neuromuscular diseases expedite translational research. *Transl Neurosci* 1:214–227.
23. Kim H, Rogers MJ, Richmond JE, McIntire SL (2004) SNF-6 is an acetylcholine transporter interacting with the dystrophin complex in Caenorhabditis elegans. *Nature* 430:891–896.
24. Hewitt JE, et al. (2018) Muscle strength deficiency and mitochondrial dysfunction in a muscular dystrophy model of *Caenorhabditis elegans* and its functional response to drugs. *Dis Model Mech* 11:dmm036137.
25. Brouilly N, et al. (2015) Ultra-structural time-course study in the C. elegans model for Duchenne muscular dystrophy highlights a crucial role for sarcomere-anchoring structures and sarcolemma integrity in the earliest steps of the muscle degeneration process. *Hum Mol Genet* 24:6428–6445.
26. Carre-Pierrat M, et al. (2006) The SLO-1 BK channel of Caenorhabditis elegans is critical for muscle function and is involved in dystrophin-dependent muscle dystrophy. *J Mol Biol* 358:387–395.
27. Mariol MC, Ségalat L (2001) Muscular degeneration in the absence of dystrophin is a calcium-dependent process. *Curr Biol* 11:1691–1694.
28. Bainbridge C, Schuler A, Vidal-Gadea AG (2016) Method for the assessment of neuromuscular integrity and burrowing choice in vermiform animals. *J Neurosci Methods* 264:40–46.
29. Beron C, et al. (2015) The burrowing behavior of the nematode Caenorhabditis elegans: A new assay for the study of neuromuscular disorders. *Genes Brain Behav* 14: 357–368.
30. Brenner S (1974) The genetics of Caenorhabditis elegans. *Genetics* 77:71–94.
31. Wang X, Schwarz TL (2009) The mechanism of Ca2+ -dependent regulation of kinesin-mediated mitochondrial motility. *Cell* 136:163–174.
32. Dagda RK, et al. (2009) Loss of PINK1 function promotes mitophagy through effects on oxidative stress and mitochondrial fission. *J Biol Chem* 284:13843–13855.
33. Oh KH, Kim H (2013) Reduced IGF signaling prevents muscle cell death in a Caenorhabditis elegans model of muscular dystrophy. *Proc Natl Acad Sci USA* 110: 19024–19029.
34. Bakker JPJ, De Groot IJM, Beelen A, Lankhorst GJ (2002) Predictive factors of cessation of ambulation in patients with Duchenne muscular dystrophy. *Am J Phys Med Rehabil* 81:906–912.
35. Bushby K, et al.; DMD Care Considerations Working Group (2010) Diagnosis and management of Duchenne muscular dystrophy, part 1: Diagnosis, and pharmacological and psychosocial management. *Lancet Neurol* 9:77–93.
36. Cyrulnik SE, Fee RJ, De Vivo DC, Goldstein E, Hinton VJ (2007) Delayed developmental language milestones in children with Duchenne's muscular dystrophy. *J Pediatr* 150: 474–478.
37. Eagle M, et al. (2002) Survival in Duchenne muscular dystrophy: Improvements in life expectancy since 1967 and the impact of home nocturnal ventilation. *Neuromuscul Disord* 12:926–929.
38. Vallejo-Illarramendi A, Toral-Ojeda I, Aldanondo G, López de Munain A (2014) Dysregulation of calcium homeostasis in muscular dystrophies. *Expert Rev Mol Med* 16: e16.
39. Rittler MR (2002) Sarcoplasmic reticulum calcium handling in maturing skeletal muscle from two models of dystrophic mice. PhD dissertation (Virginia Polytechnic Institute and State University, Blacksburg, VA).
40. Conte D, MacNeil LT, Walhout AJM, Mello C (2015) RNA interference in Caenorhabditis elegans. *Curr Protoc Mol Biol* 109:26.3.1–26.3.30.
41. Chakkalakal JV, Michel SA, Chin ER, Michel RN, Jasmin BJ (2006) Targeted inhibition of Ca2+/calmodulin signaling exacerbates the dystrophic phenotype in mdx mouse muscle. *Hum Mol Genet* 15:1423–1435.
42. Niebroj-Dobosz I, Kornguth S, Schutta HS, Siegel FL (1989) Elevated calmodulin levels and reduced calmodulin-stimulated calcium-ATPase in Duchenne progressive muscular dystrophy. *Neurology* 39:1610–1614.
43. Imbert N, Cognard C, Duport G, Guillou C, Raymond G (1995) Abnormal calcium homeostasis in Duchenne muscular dystrophy myotubes contracting in vitro. *Cell Calcium* 18:177–186.
44. Shen Y, et al. (2002) Physiological calcium concentrations regulate calmodulin binding and catalysis of adenylyl cyclase exotoxins. *EMBO J* 21:6721–6732.
45. Grange RW, Call JA (2007) Recommendations to define exercise prescription for Duchenne muscular dystrophy. *Exerc Sport Sci Rev* 35:12–17.
46. Vidal-Gadea A, et al. (2011) Caenorhabditis elegans selects distinct crawling and swimming gaits via dopamine and serotonin. *Proc Natl Acad Sci USA* 108: 17504–17509.
47. Pierce-Shimomura JT, et al. (2008) Genetic analysis of crawling and swimming locomotory patterns in C. elegans. *Proc Natl Acad Sci USA* 105:20982–20987.
48. Krajacic P, Shen X, Purohit PK, Arratia P, Lamitina T (2012) Biomechanical profiling of Caenorhabditis elegans motility. *Genetics* 191:1015–1021.
49. Rabets Y, Backholm M, Dalnoki-Veress K, Ryu WS (2014) Direct measurements of drag forces in C. elegans crawling locomotion. *Biophys J* 107:1980–1987.
50. Johari S, Nock V, Alkaisi MM, Wang W (2013) On-chip analysis of C. elegans muscular forces and locomotion patterns in microstructured environments. *Lab Chip* 13: 1699–1707.
51. Hartman JH, et al. (2018) Swimming exercise and transient food deprivation in Caenorhabditis elegans promote mitochondrial maintenance and protect against chemical-induced mitotoxicity. *Sci Rep* 8:8359.
52. Laranjeiro R, Harinath G, Burke D, Braeckman BP, Driscoll M (2017) Single swim sessions in C. elegans induce key features of mammalian exercise. *BMC Biol* 15:30.
53. Schoenfeld BJ (2010) The mechanisms of muscle hypertrophy and their application to resistance training. *J Strength Cond Res* 24:2857–2872.
54. Paul AC, Rosenthal N (2002) Different modes of hypertrophy in skeletal muscle fibers. *J Cell Biol* 156:751–760.
55. Deconinck AE, et al. (1997) Utrophin-dystrophin-deficient mice as a model for Duchenne muscular dystrophy. *Cell* 90:717–727.
56. Rieff HI, et al. (2016) The muscular dystrophy coordinating committee action plan for the muscular dystrophies. *Muscle Nerve* 53:839–841.
57. Millay DP, et al. (2009) Calcium influx is sufficient to induce muscular dystrophy through a TRPC-dependent mechanism. *Proc Natl Acad Sci USA* 106:19023–19028.
58. Blaauw B, et al. (2010) Eccentric contractions lead to myofibrillar dysfunction in muscular dystrophy. *J Appl Physiol (1985)* 108:105–111.